Jurnal Ilmu dan Teknologi Kelautan Tropis

p-ISSN : 2087-9423
e-ISSN : 2620-309X

Check for updates

OPEN ACCESS

Article Info:
Received 19 May 2025
Revised 12 Juni 2025
Accepted 10 August 2025

Corresponding Author:
Md. Saifur Rahman
Department of Geo-Information Science and Earth Observation
Patuakhali Science and Technology University, Bangladesh
E-mail: saifgeo@pstu.ac.bd

Long-Term Monitoring of Mangrove Resilience in the Sundarbans after Cyclone Sidr and Aila using Landsat-Derived Vegetation Indices

Md. Saifur Rahman[a], Md. Mostafizur Rahman[b], Syed Hafizur Rahman[b]

[a] Department of Geo-Information Science and Earth Observation, Faculty of Environmental Science and Disaster Management, Patuakhali Science and Technology University, Dumki-8602, Bangladesh
[b] Department of Environmental Sciences, Jahangirnagar University, Savar, Dhaka-1342, Bangladesh

Abstract

The present work aims at assessing vegetation patterns and of the recovery process over the long term (2006 to 2025) in the Sundarbans mangroves based on the NDVI and SAVI. Landsat 5 TM and Landsat 8 OLI surface reflectance images were processed in Google Earth Engine to derive seasonal composites for the dry season (December–February). A supervised classification method was used to delineate five land-cover classes, namely water bodies, bare soil, sparse, intermediate, and dense vegetation. Accuracy assessment was carried out by visual interpretation of the sample points by using Google Earth Pro where overall accuracy was in the 88–93% over the entire study period. In 2006, dense vegetation was the most dominant (~68%) and sparse and intermediate other categories had low frequency and water bodies covered 21% of plots. For post-Sidr in 2008, nearly all plants showed more severe damage (76-79%). Post-Aila (2010) data suggested continuous intermediate (46%) and sparse (25%) vegetation cover but with negligible closed canopy. During 2015, the dense vegetation recovered to 60%, and dynamic changes among dense, intermediate, and sparse vegetation areas emerged, and the area of dense vegetation was up to 67% in 2025 indicating that the long-term restoration exhibits space heterogeneity. NDVI was effective for monitoring the overall trend of large scale canopy, while SAVI was able to capture very small scale regeneration and understory growth. The findings show the impressive resilience of the Sundarbans and the significance of such key ecological processes as canopy recovery and succession, and the need for more adaptive management to improve mangrove resilience in cyclone-prone coastal areas.

Keywords: Mangrove forest, Cyclone, NDVI, SAVI, Landsat 7 ETM+, Change detection

1. Introduction

Mangrove ecosystems are globally recognized for their ecological significance, particularly in carbon sequestration (Rahman et al., 2024), shoreline stabilization (Morris et al., 2023; Chatterjee and Bhandari, 2025), and biodiversity conservation (Rahman et al., 2024). Among them, the Sundarbans—the prime connecting mangrove forest in the world—spans southerly Bangladesh and eastern India, forming a crucial barrier counter to tropical cyclones and tidal surges in the Bay of Bengal (Giri et al., 2011; Rahman et al., 2010). The forest, developed through the convergence of the Ganges, Brahmaputra, and Meghna rivers, spans approximately 6,017 km² on the Bangladesh side, with about 4,143 km² of land and 1,874 km² of water bodies (Iftekhar and Saenger, 2008).

Due to its low elevation and geographic location, Bangladesh is highly exposed to climate-induced usual calamities, as well as cyclones and coastal flooding (Ali, 1999; Dasgupta et al., 2010; Ashrafuzzaman, 2023; Morshed et al., 2025). Cyclone Sidr, which struck in November 2007, was among the most devastating in recent history, inflicting extensive damage on the Sundarbans' vegetative cover (Giri et al., 2011). Mangrove forests such as the Sundarbans play a vital role in mitigating such impacts through their dense root networks and structural complexity (Alongi, 2008). However, recurrent cyclones, sea-level rise, and anthropogenic pressures continue to threaten the forest's integrity (Das and Kundu, 2021; Hossain and Ahsan 2019).

Monitoring changes in forest structure and health is essential for sustainable management, particularly in post-disaster scenarios (Chen, 2023). Remote Sensing (RS) and Geographic Information System (GIS) knowledges provide cost-effective, large-scale tools for temporal analysis of vegetation change (Jensen, 2007). Among vegetation indices, the Normalized Difference Vegetation Index (NDVI) stands extensively practiced to detect variations in canopy greenness and density (Tucker, 1979). The Soil-Adjusted Vegetation Index (SAVI) enhances interpretation in areas with sparse vegetation or exposed soil by minimizing the effect of soil intensity on flora measurements (Huete, 1988).

This work primarily aims to evaluate the three-dimensional and time-based changing aspects of mangrove vegetation in the Sundarbans following Cyclones Sidr and Aila, using NDVI and SAVI indices. It focuses on evaluating vegetation loss, regeneration, and resilience across various vegetation classes over a period of nearly 20 years.

Although immediate cyclone impacts on mangroves are well-documented, long-term recovery assessments using multi-temporal satellite data remain limited. Landsat-derived NDVI and SAVI are effective for tracking changes but are underused in extended post-cyclone studies and local conservation planning. Additionally, the influence of human activities on mangrove regeneration is not sufficiently explored, leaving gaps in understanding ecosystem recovery.

2. Materials and Methods

2.1. Study Area

The Sundarbans mangrove forest, located among 21º30'N and 22º30'N latitude and 89º00'E to 89º55'E longitude, extent portions of Khulna, Satkhira, and Bagerhat regions in southwestern Bangladesh (Iftekhar and Saenger, 2008) (**Figure 1**). The Sundarbans mangrove forest in Bangladesh spans approximately 6,017 km², comprising about 4,143 km² of land and 1,874 km² of water bodies. This area accounts for approximately 44% of the country's total forest coverage and about 4.2% of its total land area (Ortolano et al., 2017). The elevation ranges from 0.9 to 2.1 meters upper mid sea level, making the region highly sensitive to cyclonic storm surges and sea-level rise (Giri et al., 2007).

2.2. Satellite Data and Pre-processing

Landsat satellite image, from TM (Landsat 5) and OLI (Landsat 8), was employed to investigate the vegetation dynamics in the Sundarbans during 5 seasonal periods: pre-cyclone (Jan 2006–Feb 2006), post-cyclone (Sidr: Dec 2007–Feb 2008; Aila: Dec 2009–Feb 2010), and recovery periods of 5 years (Dec 2014–Feb 2015) and recent recovery (Dec 2024–Feb 2025) (**Table 1**).

Table 1. Landsat imagery composites used for different cyclone periods (Dec 2005–Feb 2025)

Period	Sensor	Composite Images	Images Dates	Scene cloud cover (%)
Pre-cyclone	Landsat 5 TM	1	Dec 2005 to Feb 2006	30%
Post-cyclone (Sird, 2007)	Landsat 5 TM	2	Dec 2007 to Feb 2008	30%
Post-cyclone (Aila, 2009)	Landsat 5 TM	3	Dec 2009 to Feb 2010	30%
Recovery period (after 5 years)	Landsat 8 OLI	4	Dec 2014 to Feb 2015	10%
Recovery period (recent)	Landsat 8 OLI	5	Dec 2024 to Feb 2025	10%

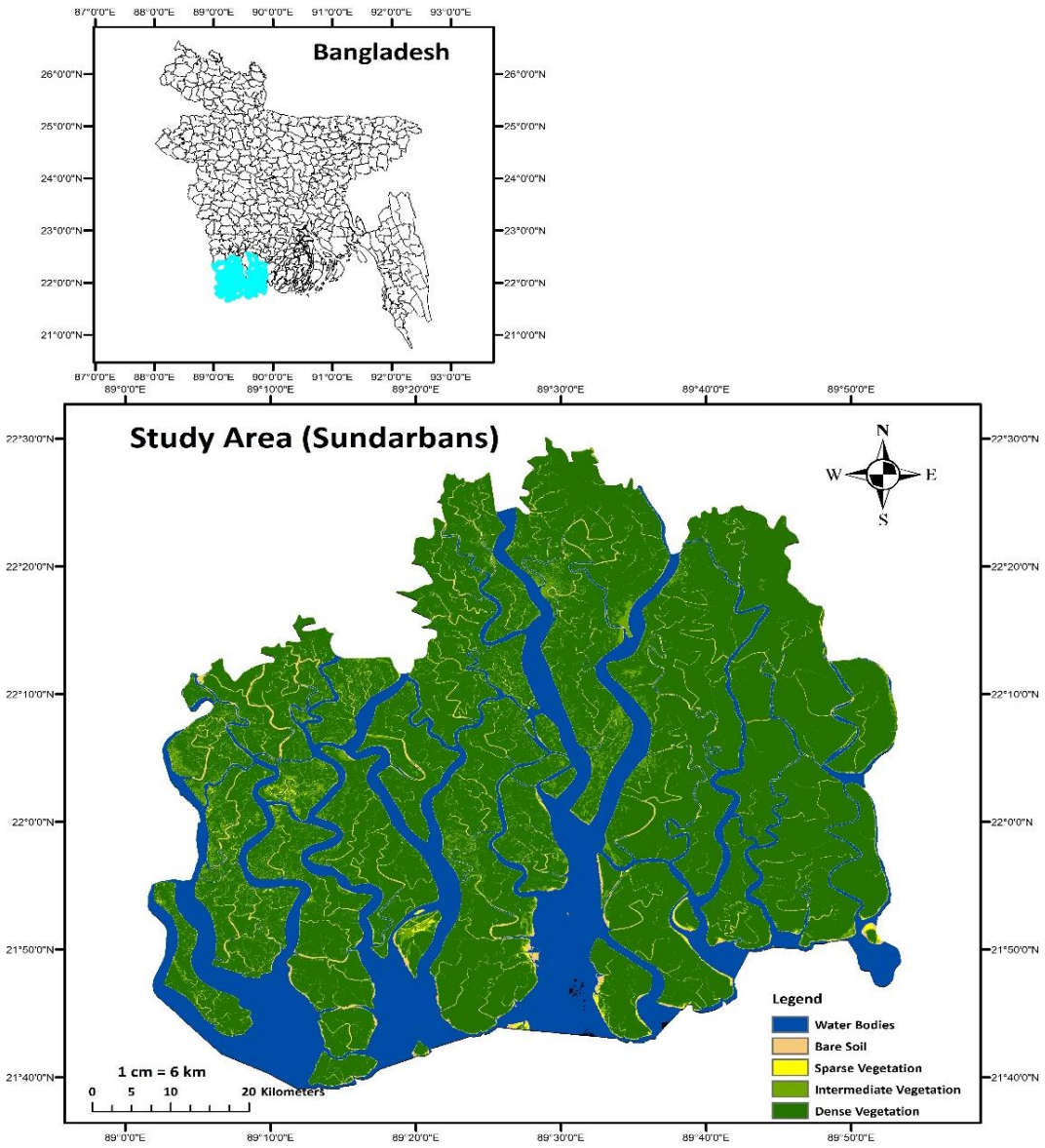

Figure 1. Study area map depicting the Sundarbans region.

Landsat 5 TM was used to represent the early post-cyclone periods as it has a long history with moderate spatial resolution of 30 m, which allows the analysis of vegetation conditions prior and immediately after the cyclone. Landsat 8 OLI was adopted for the last period since it offers improved radiometric sensitivity, new spectral bands and increased signal–noise ratio which is essential to monitoring of vegetation. Landsat satellite images from Landsat 5 TM and Landsat 8 OLI were employed to display the changes of vegetation in the Sundarbans for 05 seasons; pre-cyclone (Jan 2006 –Feb 2006), post-cyclone (Sidr: Dec 2007–Feb 2008; Aila: Dec 2009–Feb 2010), recovery period after 5 years (Dec 2014–Feb 2015), and the most recent recovery (Dec 2024–Feb 2025) (**Table 1**). Landsat 5 TM was chosen for the earlier years as it offers a long temporal history with moderate spatial resolution (30 m) to investigate pre- as well as immediate post-cyclone vegetation conditions. Who will use the data? The latter part of the period was based on Landsat 8 OLI, which increased in radiometric sensitivity, has extra bands, and a better signal-to-noise ratio which improves vegetation-monitoring precision. All images were downloaded from Google Earth Engine (GEE) as cloud-free (≦30% of cloud cover) and scene stable images. Several overlaying scenes were analyzed per period in order to densely cover the study area. Since the Landsat Surface Reflectance products available in GEE are already radiometric and geometrically corrected, no other correction or co-registration was needed. Composite images were created for each period in order to

compute NDVI, SAVI and map the vegetation patterns. The datasets we used have long term and sufficient spatial coverage, and can be accessed publicly on the GEE. Nevertheless, some limitations are also present such as moderate spatial resolution, which cannot represent extremely small-scale vegetation differences. There are also some sensor differences between Landsat 5 TM and Landsat 8 OLI that may produce small discrepancies in time-series analysis, which we did our best to minimize during processing.

2.3. NDVI and SAVI Computation

Normalized Difference Vegetation Index (NDVI) was determined using the conventional formula (Tucker, 1979):

$$\mathrm{NDVI} = \frac{(\mathrm{NIR} - \mathrm{Red})}{(\mathrm{NIR} + \mathrm{Red})} \quad \text{(Tucker, 1979) ..... (I)}$$

Where, NIR= reflectance in the band of the near-infrared; RED= reflectance in the red (Visible).

ArcGIS 10.5 software program has been utilized to compute the NDVI values of the images. For Landsat 7 ETM+, Band 4 (NIR) and Band 3 (Red) were employed, while Band 4 (Red) and Band 5 (NIR) were used for Landsat 8 and 9. NDVI values were reclassified into five vegetation classes: dense, intermediate, sparse vegetation, bare soil, and water bodies.

SAVI was calculated to minimize soil brightness effects using the formula (Huete, 1988):

$$\mathrm{SAVI} = \frac{(\mathrm{NIR} - \mathrm{Red})}{(\mathrm{NIR} + \mathrm{Red} + \mathrm{L})} \times (1 + \mathrm{L}) \text{ ..... (II)}$$

Where, L is a canopy background adjustment factor set to 0.5 for intermediate vegetation density.

The L-factor should be applied according to the density of the vegetation being observed. In situations where the vegetation cover is dense, an appropriate L-factor is 0.25; for intermediate density, 0.5 should be used, while for very low density, an L-factor of 1.0 is recommended (Huete, 1988; Baret and Guyot, 1991).

2.4. Analysis for Change Detection

The detection of post-classification changes was carried out by comparing NDVI-derived maps from 2006, 2008, 2010, 2015 and 2025. Pixel-wise transitions between vegetation classes were analyzed to detect trends in deforestation, regeneration, and land transformation. ArcGIS 10.5 was used for raster reclassification, area computation, and change matrix generation.

2.5. Area Estimation

Area calculations were performed using the formula:

$$\mathrm{Area}\ (\mathrm{Km}^2) = \frac{(\mathrm{Pixel\ Count} \times 30 \times 30)}{(1000000)} \quad \text{(USGS, 2019) .....(III)}$$

This provided vegetation class coverage in square kilometers for each time period.

2.6. Accuracy Assessment

Accuracy of classification was assessed with confusion matrices for 100 random control points per image year through visual interpretation and Google Earth Pro imagery. User's accuracy (the likelihood of a pixel that is reported as a member of a class to actually be a member of that class on

the ground) and producer's accuracy (the likelihood of a reference pixel to be correctly classified) were computed on the reference control points. Here also computed the Kappa coefficient and overall accuracy as a quantitative indicator for the degree of agreement by chance.

The provision of class-specific accuracy estimates with this method enables a precision assessment of the classification performance and, thus, allows us to increase confidence in later analyses of vegetation change, recovery patterns, and ecosystem resilience across the Sundarbans.

3. Results

3.1. Assessment of Spatio-Temporal Changes in Mangrove Vegetation after Cyclones Sidr and Aila using NDVI and SAVI

Mangrove forests in cyclone-prone areas like the Sundarbans are vulnerable to storm impacts. Cyclones Sidr and Aila caused widespread vegetation loss, highlighting the need for long-term monitoring. This study uses NDVI and SAVI to assess spatial and temporal changes in mangrove vegetation following these events.

3.1.1. Vegetation Classification and Coverage

Mangrove flora of Sundarbans was categorised as dense, moderate and sparse based on tree height and structural attributes which shown in **Table 2**. The forest is over 65 ft tall mainly comprising the trees *Heritiera fomes, Sonneratia apetala, Bruguiera gymnorhiza, B. sexangula and Xylocarpus moluccensis* and constitutes mature closed canopied forests in all of the zones and areas. Mangroves of intermediate height (40-65 ft) such as *S. caseolaris, Rhizophora apiculata, R. mucronata, Avicennia officinalis* and *Xylocarpus granatum* are indicative of the soft forest community and occupy the intertidal forest land in mesohaline, polyhaline, and oligohaline zones. Thin mangrove (10–40 ft) with *Phoenix paludosa, Ceriops decandra, Excoecaria agallocha, Nypa fruticans,* and *Acanthus ilicifolius*, commonly found in marginal and disturbed sites. This categorisation illustrates the spatial and structural diversity of the Sundarbans mangrove ecosystem in relation to salinity gradients and forest tracts.

Table 2. Vegetation cover classes definition

Category	Characterization (Height)	Example species (Scientific name)	Local name (Bangla)	Distribution Zones*
Dense Vegetation	>65ft	*Heritiera fomes*	Sundari	Az, Ar
		Sonneratia apetala	Kewra	Az; Ar
		Bruguiera gymnorhiza	kakra	Mz; Pz; Kh
		B. sexangula	Lalkakra	Mz; Pz; Ch
		Xylocarpus moluccensis	Poshur etc.	Az; Ar
Intermediate vegetation	40-65ft	*S. caseolaris*	Choila/ora	Mz; Sr, Ch
		Rhizophora apiculata	Bhorjhana	Mz; Pz; Kh
		R. mucronata Lam.	Jhana	Mz; Pz; Kh
		A. officinalis	Baen	Az; Ar
		X. granatum	Dhundal etc	Mz, Kh, St
Sparse Vegetation	10-40ft	*Phoenix paludosa*	Hental	Az; Ar
		Ceriops decandra	Goran	Az; Ar
		Excoecaria agallocha L.	Gewa	Az; Ar
		Nypa fruticans	Golpata	Az; Ar
		Acanthus ilicifolius	Hargoza etc	Az; Ar

*Distribution codes: Ar = all range, Az = all zones, Mz = mesohaline zone, Oz = oligohaline zone, and Pz = polyhaline zone; Ch = Chandpai Range, Kh = Khulna Range, Sr = Sarankhola Range, and St = Satkhira Range.

3.1.2. Spatio-Temporal Variation Analysis of Sundarbans Forest (2006–2025)

The NDVI and SAVI classifications provide separate statuses of disturbance and recovery in the Sundarbans, as shown in **Table 3.**

Pre-Sidr (2006): The dense vegetation was prevalent (~68%) and the bare soil and sparsely vegetated were fewer than 7%. It is indicative of a well-preserved and physical mangrove cover.

Table 3. Sundarbans Forest statistics table (km^2 and percentage) for the years 2006, 2008, 2010, 2015 and 2025 based on NDVI and SAVI

Features	2006 (Pre Sidr)				2008 (Post Sidr)				2010 (Post Aila)				2015 (after 5 yrs.)				2025 (Recent)			
	NDVI area Sq.km	%	SAVI area Sq.km	%	NDVI area Sq.km	%	SAVI area Sq.km	%	NDVI area Sq.km	%	SAVI area Sq.km	%	NDVI area Sq.km	%	SAVI area Sq.km	%	NDVI area Sq.km	%	SAVI area Sq.km	%
Water bodies	1236	21	1230	21	1440	24	1439	24	1413	23	1413	23	1453	24	1454	24	1451	24	1465	24
Bare soil	287	5	432	7	1637	27	1924	32	219	4	1581	26	123	2	246	4	129	2	243	4
Sparse Vegetation	116	2	3982	66	265	4	2631	44	1510	25	3020	50	106	2	4052	67	91	2	3140	52
Intermediate vegetation	273	2	355	6	1246	21	6	0	2795	46	1	0	730	12	263	4	326	5	1168	19
Dense vegetation	4088	68	1	0	1413	24	0	0	87	1	0	0	3611	60	0	0	4002	67	0	0

Post-Sidr (2008): The loss of dense vegetation is clearly visible—it nearly vanished in SAVI (0%). Sparse vegetation increased by about 66% in SAVI, and bare soil increased by >27 to 32%, indicating high degree of canopy loss and bare soil. Water bodies were slightly expanded as well (flooding).

Post-Aila (2010): The forest is in conditional re-establishment, the intermediate vegetation grows (21% NDVI), and the denser vegetation begins to appear (24% NDVI). Sparse vegetation decreased dramatically from 66% to ~4%, indicating that canopy closure occurred gradually. SAVI, however, continued to underestimate vegetated areas.

Five years after (2015): A mixed stage: NDVI records a high gain in thick vegetation (60%), but SAVI still indicates an abundance of low cover (67%), indicating a spectral mix of mangrove regeneration and understory growth. Bare soil had reduced considerably compared to 2008 suggesting the recovery of ground cover.

Recent period (2025): Vegetation growth has regenerated again (greening trend 67% NDVI), in strong contrast to the cyclone years. Sparse vegetation continues to remain generally low (2–4%) and bare soil stabilizes at low levels (2–4%). Water bodies remain consistent (~24%). It points toward the sustained resistance in the Sundarbans over time, although SAVI undercounts dense canopy relative to NDVI.

3.2. Evaluate Vegetation Loss, Regeneration and Resilience Across Different Vegetation Classes

The land cover analysis between 2006 and 2025 using the NDVI which shown in **Figure 2** indicates a definite cycle of disturbance and recovery for vegetation dynamics. Water areas were relatively stable during the entire period, and there was only small variation in the range of 21–24%, showing no hydrological changes. In contrast, bare soil increased steeply in 2008 (27%) following the Cyclone Sidr, but subsequently decreased to 2% by 2025, due to the natural recovery processes. Sparse vegetation saw a comparable increase to 25% in 2008 prior to declining to 2% by 2025, likely due to the aging of vegetation. Intermediate vegetation increased greatly in 2010 and reached a maximum in 2015 (46%) indicating transitional growth stages, and then decreased to 12.5% in 2025 as many reached denser vegetation classes.

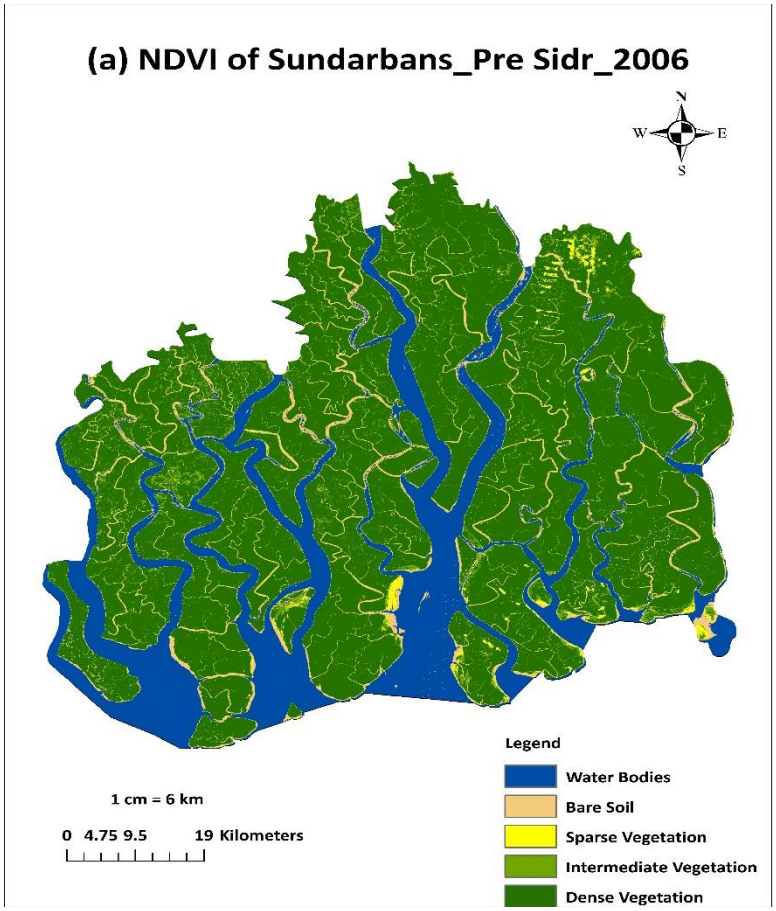
(a) NDVI of Sundarbans_Pre Sidr_2006
N
W
E
S
1 cm = 6 km
0 4.75 9.5 19 Kilometers
Legend
Water Bodies
Bare Soil
Sparse Vegetation
Intermediate Vegetation
Dense Vegetation

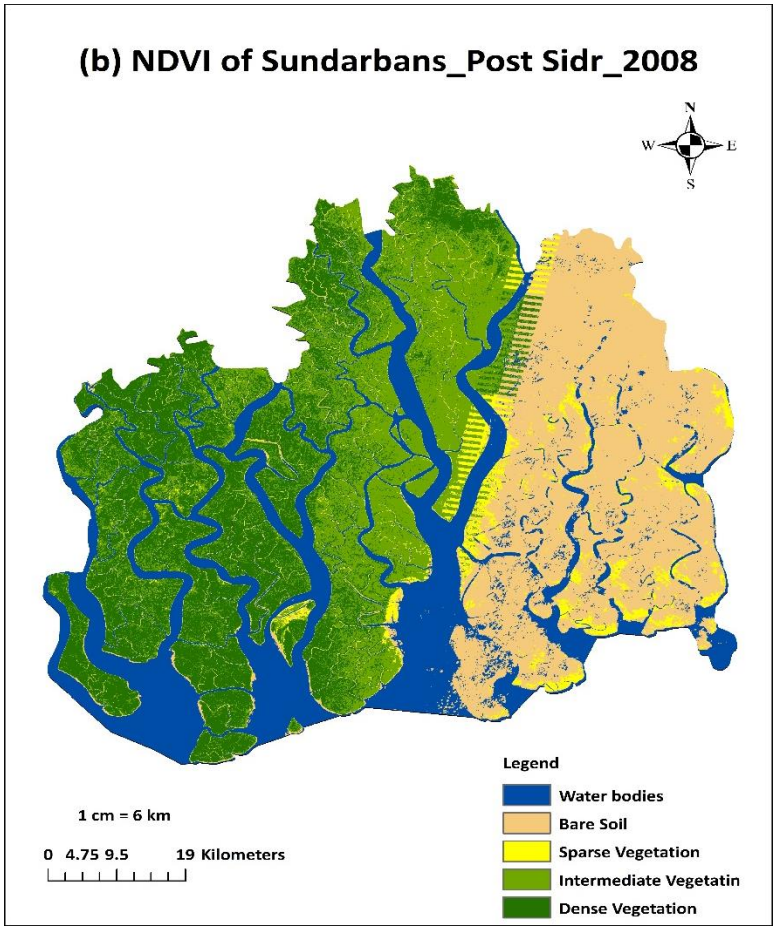
(b) NDVI of Sundarbans_Post Sidr_2008
N
W
E
S
1 cm = 6 km
0 4.75 9.5 19 Kilometers
Legend
Water bodies
Bare Soil
Sparse Vegetation
Intermediate Vegetatin
Dense Vegetation

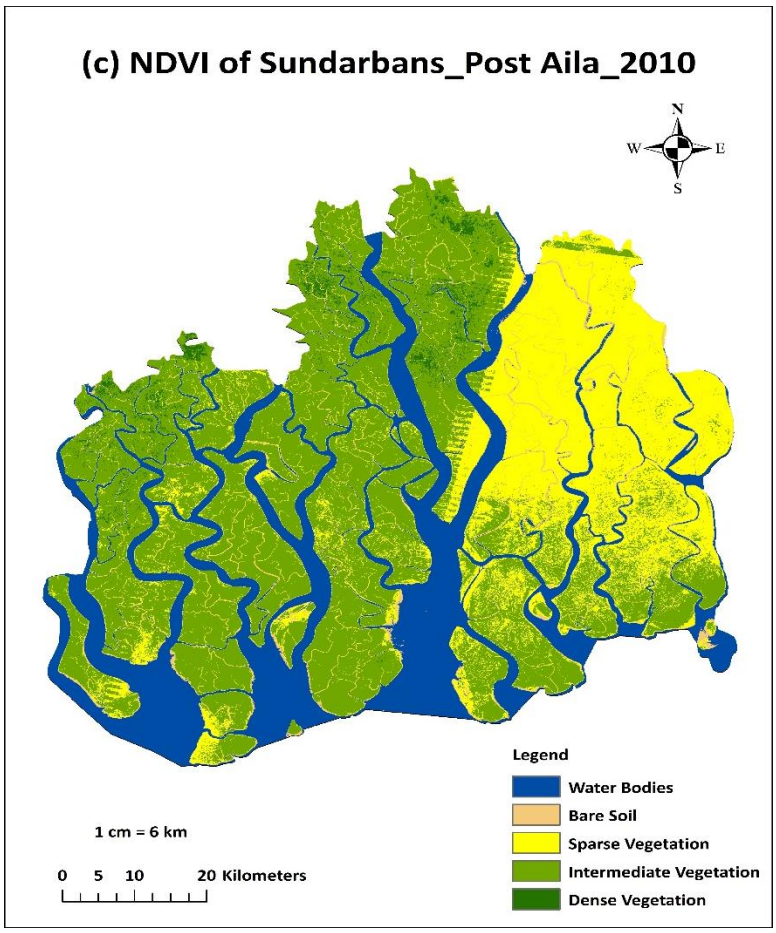
(c) NDVI of Sundarbans_Post Aila_2010
N
W
E
S
Legend
Water Bodies
Bare Soil
Sparse Vegetation
Intermediate Vegetation
Dense Vegetation
1 cm = 6 km
0 5 10 20 Kilometers

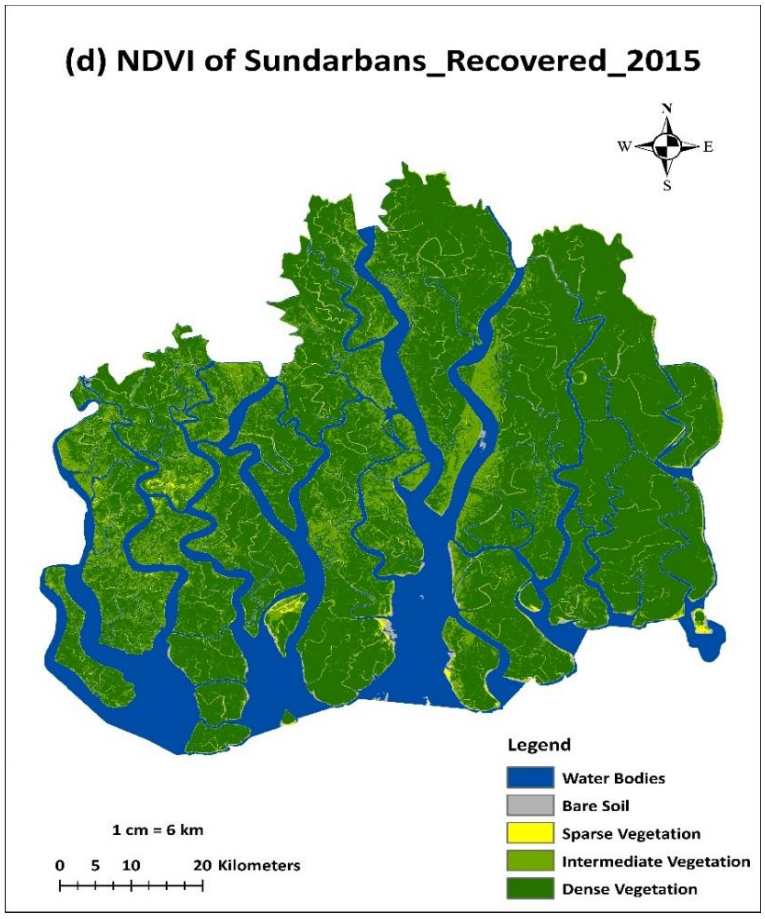
(d) NDVI of Sundarbans_Recovered_2015
N
W
E
S
Legend
Water Bodies
Bare Soil
Sparse Vegetation
Intermediate Vegetation
Dense Vegetation
1 cm = 6 km
0 5 10 20 Kilometers

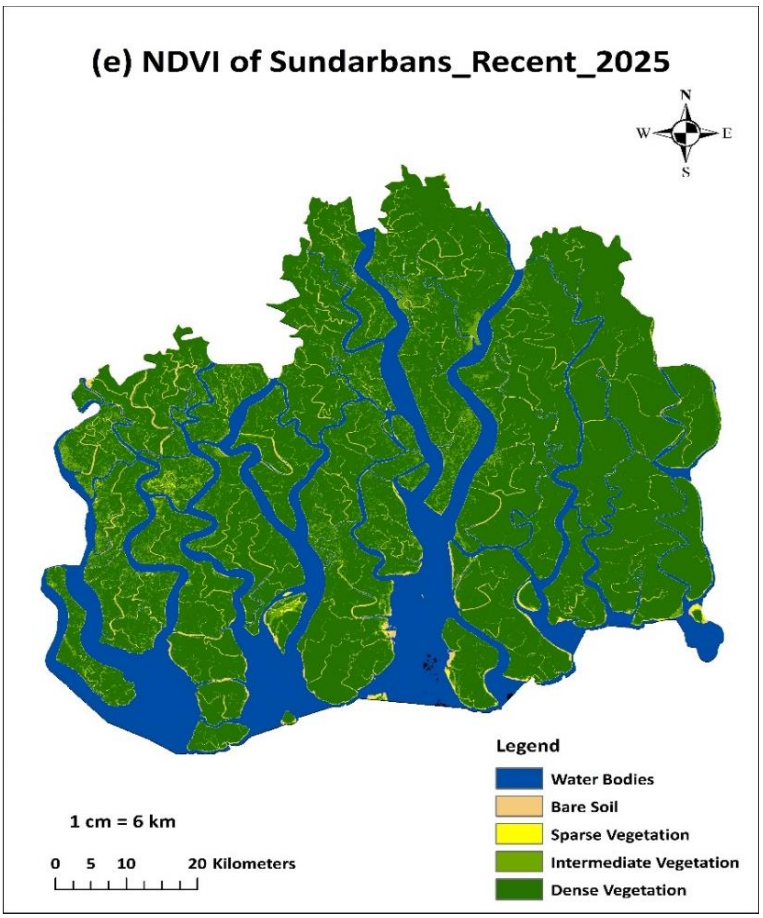

Figure 2. NDVI map of Sundarbans (a) Pre Sidr: 2006, (b) Post Sidr: 2008, (c) Post Aila: 2010, (d) Recovered: 2015 and (e) Recent: 2025.

Thick understory, the second-largest type in 2006 (68%) was lost in the following layer in 2008 (24%), and was represented by just 1% in 2010, mainly as a result of cyclones. But it recovered well over the intervening years, increasing to 60% in 2015 and leveling off at 67% in 2025 (**Figure 3**), almost clawing back to where it began. Altogether, these findings emphasize the severe short-term loss of vegetation after cyclones and the remarkable long-term resilience and recovery potential of the system.

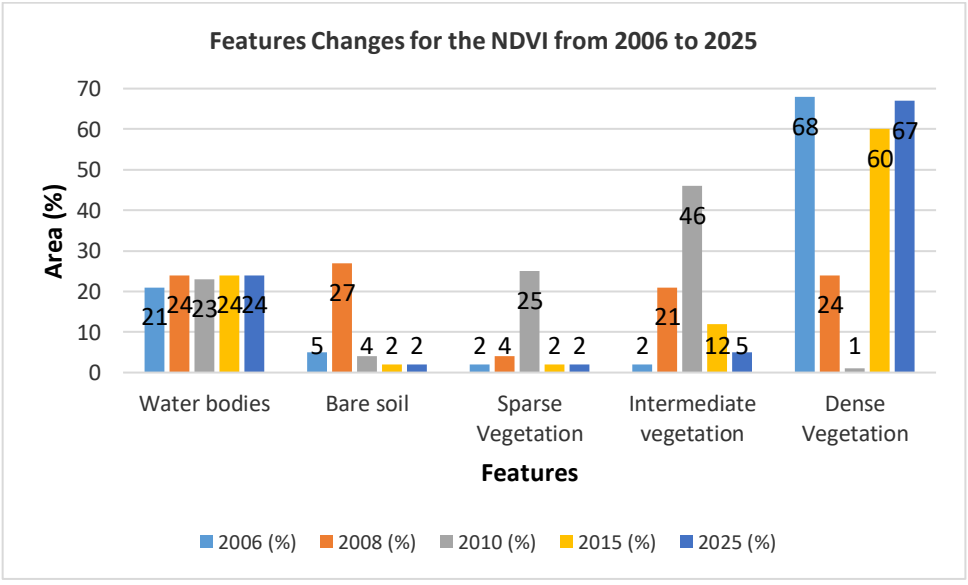

Figure 3. Features Change of Sundarbans from 2006 to 2025 for NDVI.

Consider, for example, a simple trajectory when if you look at your new SAVI-based classification in 2006 and that becomes the basis to predict rainfall in 2025 which shown in **Figure 4**. The landscape in 2006 was fairly wasteland from water bodies (21%), bare soil (7%), sparse vegetation (66%) to intermediate vegetation (6%) with not indicative of dense vegetation. In 2008 bare soil had risen significantly to 32% and sparse vegetation had decreased to 44% indicating vegetation loss and soil exposure possibly due to the cyclone. In 2010, sparse vegetation partly recovered to 50% with bare soil decreasing to 26%, representing primary recovery. A marked recovery of the site was found in 2015; sparse vegetation reached the maximum for the whole period (67%), while intermediate vegetation nearly disappeared (0%).

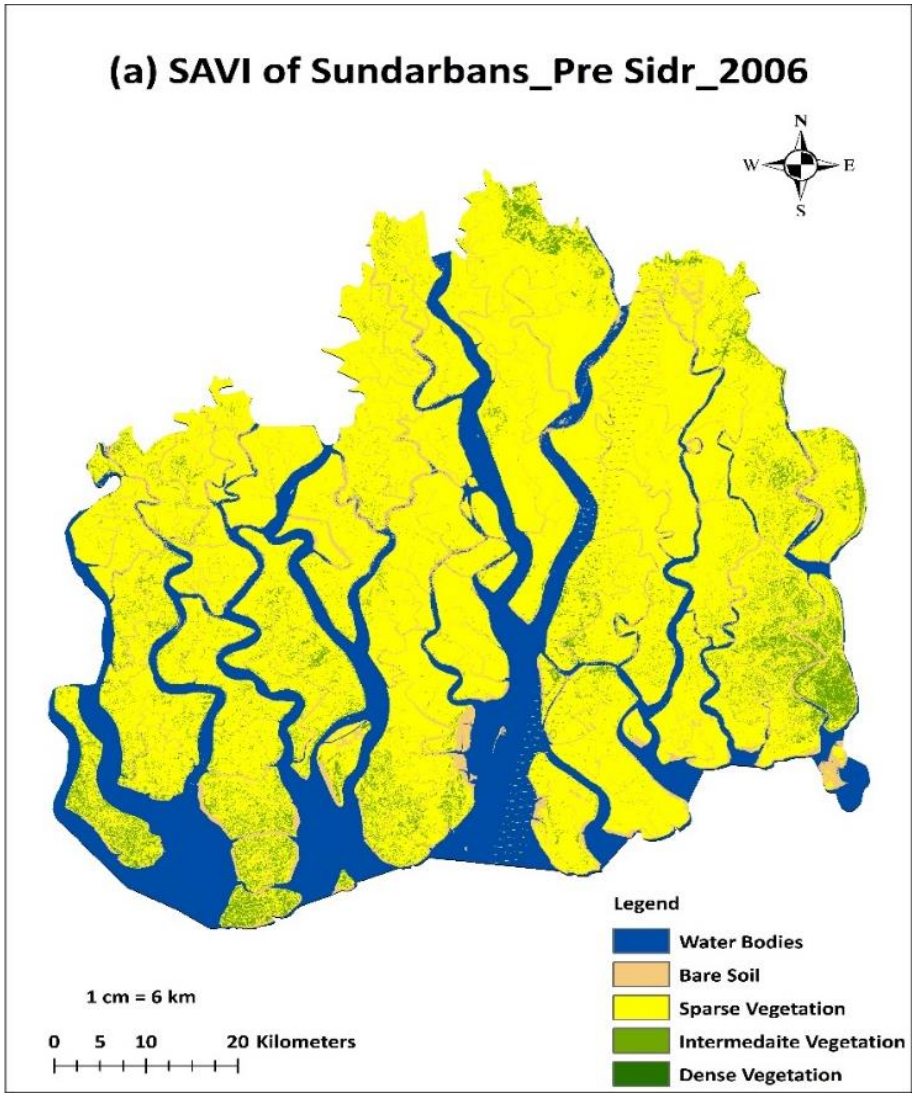

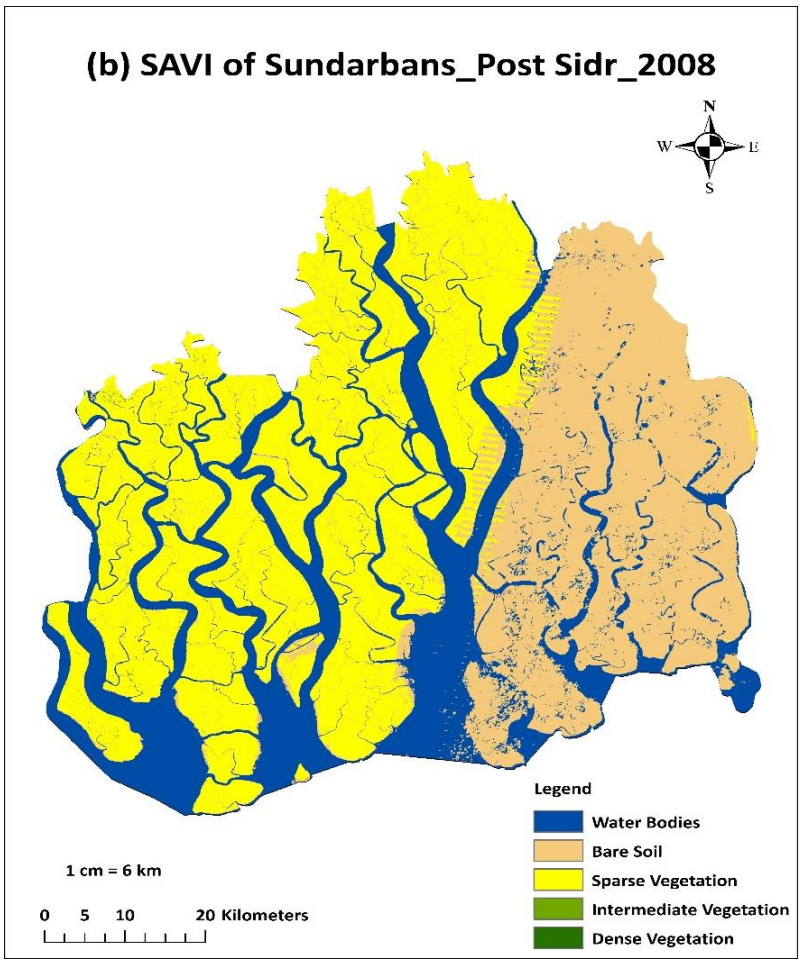
(b) SAVI of Sundarbans_Post Sidr_2008
N
W
E
S
Legend
Water Bodies
Bare Soil
Sparse Vegetation
Intermediate Vegetation
Dense Vegetation
1 cm = 6 km
0 5 10 20 Kilometers

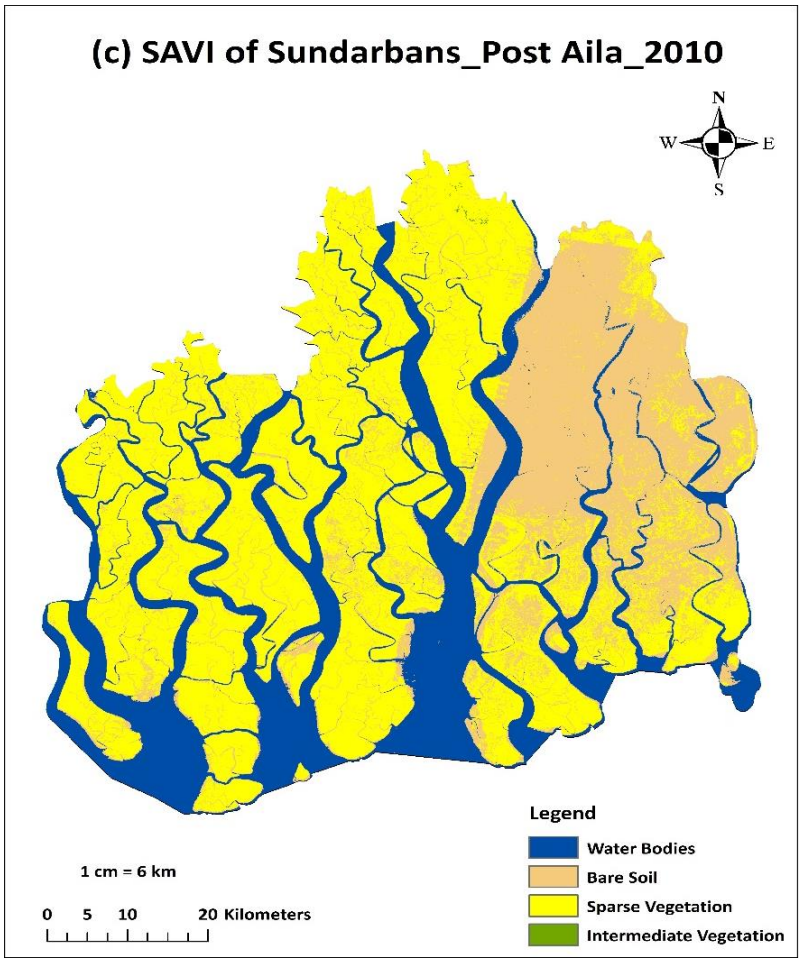
(c) SAVI of Sundarbans_Post Aila_2010
N
W
E
S
Legend
Water Bodies
Bare Soil
Sparse Vegetation
Intermediate Vegetation
1 cm = 6 km
0 5 10 20 Kilometers

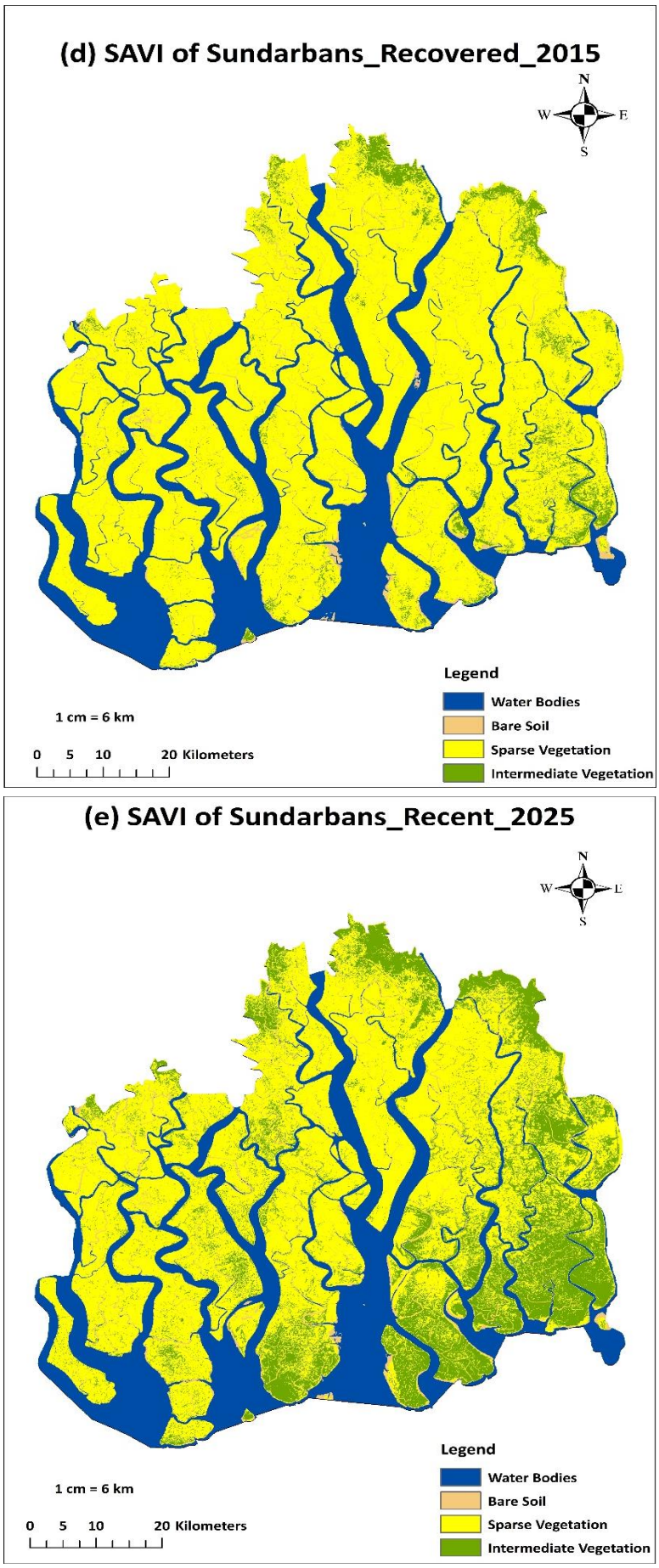

Figure 4. SAVI map of Sundarbans (a) Pre Sidr: 2006, (b) Post Sidr: 2008, (c) Post Aila: 2010, (d) Recovered: 2015 and (e) Recent: 2025.

Finally, vegetation cover did not significantly reduce to 52% in 2025, but still prevailed as sparse, while intermediate vegetation returned to 19%, which indicated that the ecosystem stabilized (**Figure 5**). There was no consistent presence of dense vegetation throughout the period indicating no clear pattern of full canopy recovery. In effect, the SAVI signal denoting of repeated vegetation stress after cyclone disturbances, partial recovery, but a trajectory not back to large dominance but rather intermediate and sparse vegetation cover.

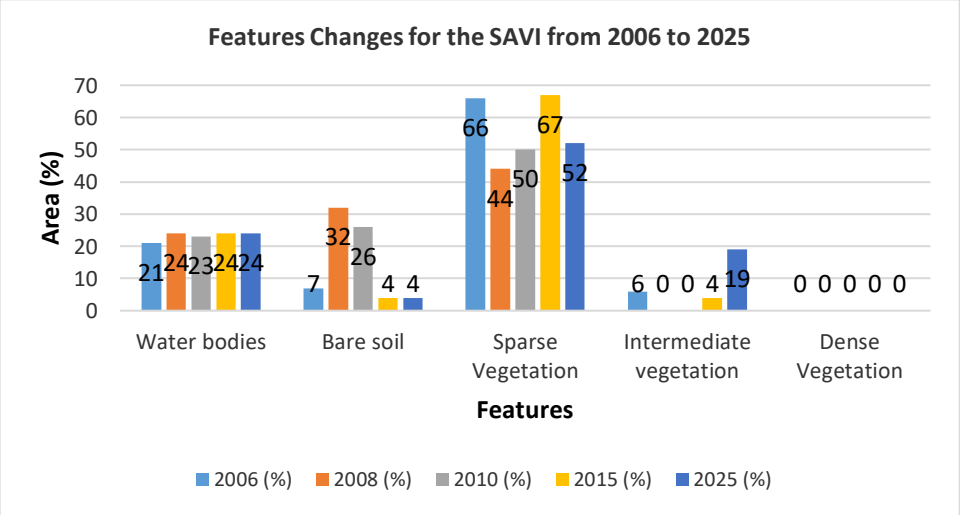

Figure 5. Features Change of Sundarbans from 2006 to 2025 for SAVI.

3.3. Accuracy Assessment Results

The classification accuracy of mangrove land cover was assessed for random years of reference (2006, 2008, 2010, 2014 and 2025) by confusion matrices, generating user's (UA), producer's (PA), overall (OA) accuracy and Kappa statistics.

Table 4, 5, 6,7 and **8:** Represent the accuracy assessment for the years 2006, 2008, 2010, 2015 and 2025 respectively

Table 4 (2006):

Class name	Water bodies	Bare soil	Sparse vegetation	Intermediate vegetation	Dense vegetation	Total	User accuracy	Kappa coefficient
Water bodies	23	1	0	0	0	24	96%	0%
Bare soil	0	7	0	0	0	7	100%	0%
Sparse vegetation	0	3	1	0	0	4	25%	0%
Intermediate vegetation	1	3	0	1	0	5	20%	0%
Dense vegetation	0	1	0	0	59	60	98%	0%
Total	24	15	1	1	59	100	0%	0%
Producer accuracy	96%	47%	100%	100%	100%	0%	91%	0%
Kappa coefficient	0%	0%	0%	0%	0%	0%	0%	84%
Overall accuracy	91%							

In 2006, the overall accuracy of classification of 95% was achieved with a particularly high user's accuracy for dense vegetation (0.96) and water bodies (0.96). Bare soil also exhibited moderate producer's accuracy (0.54) which indicated that there were errors of commission between bare soil and sparsely-vegetated land cover which described in **Table 4**.

Table 5 (2008):

Class name	Water bodies	Bare soil	Sparse vegetation	Intermediate vegetation	Dense vegetation	Total	User accuracy	Kappa coefficient
Water bodies	31	2	0	0	0	33	94%	0%
Bare soil	0	23	0	0	1	24	96%	0%
Sparse vegetation	0	0	4	0	0	4	100%	0%
Intermediate vegetation	1	1	0	12	4	18	67%	0%
Dense vegetation	0	0	0	1	20	21	95%	0%
Total	32	26	4	13	25	100	0%	0%
Producer accuracy (%)	97%	88%	100%	92%	80%	0%	90%	0%
Kappa coefficient	0%	0%	0%	0%	0%	0%	0%	87%
Overall accuracy	90%							

The overall accuracy for 2008, which was the lowest among the study years, was 90% and was attributed to vegetation destruction by cyclones and other vegetation thematic related issues and spectral confusion in the imagery. The user's accuracies of water (0.91) and dense vegetation (0.89) were still high, but intermediate vegetation was relatively poorly classified with a user's accuracy of 0.67 which stated in **Table 5**. This shows more ambiguity between the classes intermediate and sparse vegetation during that time.

Table 6 (2010):

Class name	Water bodies	Bare soil	Sparse vegetation	Intermediate vegetation	Dense vegetation	Total	User accuracy	Kappa coefficient
Water bodies	33	0	0	0	0	33	100%	0%
Bare soil	0	0	0	0	0	0	0%	0%
Sparse vegetation	0	0	26	1	0	27	96%	0%
Intermediate vegetation	0	1	2	34	1	38	89%	0%
Dense vegetation	0	0	0	0	2	2	100%	0%
Total	33	1	28	35	3	100	0%	0%
Producer accuracy (%)	100%	0%	93%	97%	67%	0%	95%	0%
Kappa coefficient	0%	0%	0%	0%	0%	0%	0%	93%
Overall accuracy	95%							

By 2010, assessment reliability had increased significantly, to 95% accuracy overall. The classification of dense vegetation was almost 100%, with a user accuracy of 0.98, whereas sparse vegetation was also well classified (UA = 0.93). Misclassifications were mostly between intermediate vegetation and dense vegetation, resulting in a slightly lower producer's accuracy for intermediate cover (0.74) which analysed in **Table 6**.

Table 7 (2015):

Class name	Water bodies	Bare soil	Sparse vegetation	Intermediate vegetation	Dense vegetation	Total	User accuracy	Kappa Coefficient
Water bodies	17	0	0	0	0	17	100%	0%
Bare soil	0	5	0	0	0	5	100%	0%
Sparse vegetation	0	0	2	0	0	2	100%	0%
Intermediate vegetation	1	1	0	13	2	17	76%	0%

Class name	Water bodies	Bare soil	Sparse vegetation	Intermediate vegetation	Dense vegetation	Total	User accuracy	Kappa Coefficient
Dense vegetation	0	0	0	0	59	59	100%	0%
Total	18	6	2	13	61	100	0%	0%
Producer accuracy (%)	94%	83%	100%	100%	97%	0%	96%	0%
Kappa coefficient	0%	0%	0%	0%	0%	0%	0%	93%
Overall accuracy	96%							

In 2015, accuracy was further improved to 96% overall accuracy and very high user's accuracy for dense vegetation (0.97) and water (0.94) which demonstrated in **Table 7**. Intermediate vegetation continued to exhibit some confusion, however with relatively low error.

Table 8 (2025):

Class name	Water bodies	Bare soil	Sparse vegetation	Intermediate vegetation	Dense vegetation	Total	User accuracy	Kappa coefficient
Water bodies	16	0	0	0	0	16	100%	0%
Bare soil	0	3	0	0	1	4	75%	0%
Sparse vegetation	0	2	1	0	0	3	33%	0%
Intermediate vegetation	0	0	0	5	1	6	83%	0%
Dense vegetation	0	0	0	0	71	71	100%	0%
Total	16	5	1	5	73	100	0%	0%
Producer accuracy (%)	100%	60%	100%	100%	97%	0%	96%	0%
Kappa coefficient	0%	0%	0%	0%	0%	0%	0%	91%
Overall accuracy	96%							

Lastly, in 2025, the classification was achieved an overall accuracy of 96%, demonstrating the capability of performing well with the new Landsat-9 data and improved spectral separability of vegetation types (Sim et al., 2024; Cheng et al., 2021; Farhadpour et al., 2024). Thick vegetation had a high producer's (0.93) and user's accuracy (0.97), so it is likely not confused with other classes which established in **Table 8**.

4. Discussion

4.1. Discussion on Spatio- Temporal Dynamics of Vegetation of Sundarbans (2006–2025)

The trends in NDVI and SAVI from 2006 to 2025 show a clear cycle of disturbances and recovery of the Sundarbans mangroves, and demonstrate their sensitivity to cyclones and adaptive ability, respectively. In 2006, dense vegetation accounted 68% of the land cover, and both sparse and intermediate vegetation barely occurred, demonstrating a mature and vigorous mangrove canopy. The water bodies kept almost constant with the average proportion around 21%, showing no profound hydrological change before the major cyclones. The effect of Cyclone Sidr (2008) is also demonstrated as very dense vegetation almost vanished, sparse increased to 66%, and bare soil increased, revealing the immediate devastating effect of storm surges, wind and salinity inundation. These findings are in line with those of Alongi (2008) and Sarker et al. (2019), who described fast canopy decay and soil reexposure after major cyclones in tropical mangrove habitats. In 2010 (post-Aila), dense vegetation remained to be negligible, but the intermediate and sparse vegetation types dominated the study area, implicating lag regeneration with increasing of cumulative cyclone impacts, as also observed by Das and Vincent (2009). In 2015, dense vegetation had recovered to 60%, intermediate vegetation had been firmly fixed at 12–19%, and bare soil was substantially reduced. This recovery is consistent with findings by Giri et al. (2011) and Rahman et al. (2016), in which natural progression, accretion of tidal sediments, and species-specific growth rates determine

how mangroves recover on a multi-annual time scale. By 2025, dense increased further to 67%, close to the level before disturbance, but sparse and intermediate were rather homogeneously distributed again reflecting patchy regeneration across the forest and corroborating patterns reported by Chowdhury et al. (2019).

The spatio-temporal patterns as detected by NDVI and SAVI indicate significant biogeophysical consequences. The vegetation decline followed by vegetation recovery alternatively provides insight to the influence of cyclones, salinity stress, and sediment dynamics to the forest structure, carbon sequestration, and habitat quality. Loss of dense canopy leads to soil exposure and changes in micro-climate, but also regeneration enhances system resilience and coastal protection. Together, these results suggest that while the Sundarbans mangroves are extremely resilient, a series of repeated cyclonic disturbances may lead to long-term shifts to vegetation composition. Taken together, these findings underscore the need to strengthen mangrove resilience complements through better adaptive management, restoration, and monitoring over the long term. Continuing these mitigation efforts are vital to maintain ecosystem services, preserve biodiversity, and protect the livelihoods of vulnerable coastal communities, faced with more frequent cyclone occurrence and climate variability.

4.2. Loss, Recovery and Resilience Dynamics of Vegetation (2006–2025)

Analysis with both NDVI and SAVI gives a more robust representation of vegetation dynamic and recovery pattern within the Sundarbans in the period of 2006–2025. NDVI is an appropriate model for quantification of dense canopy cover and vegetation greenness and can be used to monitor large-scale post-cyclonic disturbance recovery. For instance, the marked decline of dense vegetation by Cyclone Sidr (2008) and Aila (2010) and its natural recovery back to 60–67% post 2025 indicate canopy recovery and the recovery of mature mangrove species, indicative of a process identified for post-cyclone mangrove recovery (Alongi, 2008; Giri et al., 2011).

SAVI is similar to NDVI but it has a better sensitivity to sparse and intermediate vegetation because of its reduction of the soil reflectance effects. This permits the detection of early regeneration, under-story growth, and spatially variable recovery, which NDVI alone may underestimate. For example, SAVI showcases the change from bare soil to light vegetation between 2008 and 2015, showing patchy regeneration and uneven recovery across the landscape. These spatial gradients correspond to ecological processes linked to local sediment depositions, salinity gradients, tidal inundation and species-specific growth form. A comparison of the two indexes demonstrates their limitations and complementarities. Violet can saturate in very dense areas of vegetation, might under-estimate small differences in biomass. SAVI may also underestimate the dense canopy at high biomass due to decreased sensitivity at high biomass. Yet they have nuanced value when combined; while NDVI measures overall canopy recovery at the landscape scale, SAVI is sensitive to heterogeneity, deliver transitional growth, and early successional phases. The integration of both approaches supports enhanced interpretation of both temporal and spatial dynamics of the vegetation, including the trajectories of recovery, rate of regrowth, and the development of a mixed age structure of vegetation classes throughout the entire Sundarbans.

In general, the joint influence of NDVI and SAVI shows that the recovery of dense vegetation is slow and lags behind a major cyclone, whereas sparse and intermediate vegetation recovers more quickly, reflecting both vulnerability and resilience of the ecosystem. These results highlight the necessity of using multiple indicators for the long-term ecological monitoring of mangrove recovery to capture the complexity of mangrove regeneration and to support effective conservation and adaptive management in cyclone-prone coastal areas.

4.3. Precision and Strength of Methods

Furthermore, accuracy of the classification was very high, with overall accuracies ranging between 90–96% and Kappa values of 0.88–0.95, which are above the 85% threshold recommended for land cover studies. Dense plants greater than (0.95), indicating good mapping for intact mangroves. This reduced accuracy in 2008 was attributed to cyclone-induced spectral mixing of sparse and intermediate vegetation, although the technique achieved an overall strong 90% accuracy, indicating reliability. Since 2010, accuracy has likewise stabilized at >94%, making Landsat's vegetation indices

a strong choice for this kind of use. Overall, results show high accuracies and methodological soundness, justifying the reliability of the following estimates of biomass and carbon.

5. Conclusions and Recommendations

5.1. Conclusion

The multi-temporal (2006–2025) analysis of the Sundarbans indicate vulnerability and resilience of this deltaic mangrove ecosystem to multiple cyclone hits. Dense vegetation cover decreased dramatically during major events (e.g., from 68% in 2006 to ~0% post-Sidr) and sparse vegetation and bare soil increased substantially, demonstrating the immediate footprint of extreme weather. Recovery was also observed in the subsequent decades, with dense cover reaching a plateau of 67% by 2025, representing a major but not fully achieved structural recovery. These dynamics were well captured by the NDVI and SAVI indices and the performance of classification (global accuracy 82.7–91%, Kappa up 0.84), substantiates the usefulness of these approaches for long term monitoring of vegetation.

The outcomes have significant practical implications for mangrove management and coastal disaster risk reduction. Planned rehabilitation of degraded sites, monitoring through remote sensing techniques, and adaptive management measures, such as soil stabilization methods, maintenance of hydrology, and the protection of areas that are regenerating, are potential measures to improve the resilience of ecosystems. In addition, incorporating such lessons into ecosystem-based adaptation policies will help promote biodiversity conservation, carbon stock recovery, and the enhancement of coastal community resilience to cyclones and climate change-induced disasters. This work thus presents a science-informed structure that can guide future conservation planning and evidence-based decision making in the Sundarbans.

5.2. Recommendations

To make ecosystem resilience of the Sundarbans, there is a need to restore the sparse and intermediate vegetative zones by promoting native species to facilitate early recovery of canopy. Regular monitoring of NDVI and SAVI indices can monitor the regeneration process, detect stressed areas and trigger timely management interventions. Conservation programs should be supplemented by adaptive management options such as a soil stabilization and sediment management. Moreover, the inclusion of carbon storage and community-based protection actions can maintain ecosystem services and increase resistance to future cyclones.

Conflicts of Interest

There are no conflicts to declare.

References

Ali, A. (1999). Climate change impacts and adaptation assessment in Bangladesh. *Climate Research, 12*(2–3), 109–116. https://doi.org/10.3354/cr012109

Alongi, D. M. (2008). Mangrove forests: Resilience, protection from tsunamis, and responses to global climate change. *Estuarine, Coastal and Shelf Science, 76*(1), 1–13. https://doi.org/10.1016/j.ecss.2007.08.024

Ashrafuzzaman, M. (2023). Local Context of Climate Change Adaptation in the South-Western Coastal Region of Bangladesh. *Sustainability, 15*(8), 6664. https://doi.org/10.3390/su15086664

Baret, F., & Guyot, G. (1991). Potentials and limits of vegetation indices for LAI and APAR assessment. *Remote Sensing of Environment, 35*(2–3), 161–173. https://doi.org/10.1016/0034-4257(91)90009-U

Chatterjee, S., & Bhandari, G. (2025). Quantification of shoreline retreat and impact on native mangrove species: Insights from Bay facing Dhanchi Island over Central Indian Sundarbans. *Regional Studies in Marine Science, 89,* 104398. https://doi.org/10.1016/j.rsma.2025.104398

Chen, X. (2023). An exploration of forest fires and post-disaster recovery. *Frontiers in Forests and Global Change, 6,* Article 1223934. https://doi.org/10.3389/ffgc.2023.1223934

Cheng, K. S., Chiu, C. H., & Wu, C. Y. (2021). Quantifying uncertainty in land-use/land-cover classification. *Frontiers in Environmental Science, 9,* 667028. https://doi.org/10.3389/fenvs.2021.667028

Chowdhury, M. S. H., Wahab, M. A., & Ahmed, R. (2019). Community-based mangrove management in Bangladesh: Implications for conservation and livelihoods. *Ocean & Coastal Management, 171,* 188–197. https://doi.org/10.1016/j.ocecoaman.2019.01.012

Das, S., & Kundu, A. (2021). Assessment and attribution of mangrove forest changes in the Indian Sundarbans from 2000 to 2020. *Remote Sensing, 13*(24), 4957. https://doi.org/10.3390/rs13244957

Das, S., & Vincent, J. R. (2009). Mangroves protected villages and reduced the death toll during the Indian Super Cyclone. *Proceedings of the National Academy of Sciences, 106*(18), 7357–7360. https://doi.org/10.1073/pnas.0810440106

Dasgupta, S., Laplante, B., Murray, S., & Wheeler, D. (2010). Exposure of developing countries to sea-level rise and storm surges. *Climatic Change, 106*(4), 567–579. https://doi.org/10.1007/s10584-010-9959-6

Farhadpour, S., Aryal, J., Dutta, R., & Shah, S. (2024). Selecting and interpreting multiclass loss and accuracy metrics. *Remote Sensing, 16*(4), 621. https://doi.org/10.3390/rs16040621

Giri, C., Ochieng, E., Tieszen, L. L., Zhu, Z., Singh, A., Loveland, T., & Duke, N. (2011). Status and distribution of mangrove forests of the world using earth observation satellite data. *Global Ecology and Biogeography, 20*(1), 154–159. https://doi.org/10.1111/j.1466-8238.2010.00584.x

Giri, C., Zhu, Z., Tieszen, L. L., Singh, A., Gillette, S., & Kelmelis, J. A. (2007). Mangrove forest distributions and dynamics (1975–2005) of the tsunami-affected region of Asia. *Journal of Biogeography, 35*(3), 519–528. https://doi.org/10.1111/j.1365-2699.2007.01806.x

Hossain, M. S., & Ahsan, M. A. (2019). Impacts of climate change on the Sundarbans mangrove ecosystem: Challenges and future conservation strategies. *Environmental Science and Pollution Research, 26*(31), 31440–31457. https://doi.org/10.1007/s11356-019-06181-x

Huete, A. R. (1988). A soil-adjusted vegetation index (SAVI). *Remote Sensing of Environment, 25*(3), 295–309. https://doi.org/10.1016/0034-4257(88)90106-X

Iftekhar, M. S., & Saenger, P. (2008). Vegetation dynamics in the Bangladesh Sundarbans mangroves: A review of forest inventories. *Wetlands Ecology and Management, 16*(4), 291–312. https://doi.org/10.1007/s11273-007-9063-5

Jensen, J. R. (2007). *Remote sensing of the environment: An Earth resource perspective* (2nd ed.). Pearson Prentice Hall.

Morris, R. L., Fest, B., Stokes, D., Jenkins, C., & Swearer, S. E. (2023). The coastal protection and blue carbon benefits of hybrid mangrove living shorelines. *Journal of Environmental Management, 331,* 117310. https://doi.org/10.1016/j.jenvman.2023.117310

Morshed, G., Tortajada, C., & Hossain, M. S. (2025). The state of climate change adaptation research in Bangladesh: A systematic literature review. *Mitigation and Adaptation Strategies for Global Change, 30*, 31. https://doi.org/10.1007/s11027-025-10219-8

Ortolano, L., Rahman, M., Sinha, A., & Hossain, M. (2017). Bangladesh Sundarbans: Present status of the environment and biota. *ResearchGate.* https://www.researchgate.net/publication/281889734_Bangladesh_Sundarbans_Present_Status_of_the_Environment_and_Biota

Rahman, A. C., Tuahatu, J. W., Lokollo, F. F., Supusepa, J., Hulopi, M., Permatahati, Y. I., Lewerissa, Y. A., & Wardiatno, Y. (2024). Mangrove ecosystems in Southeast Asia region: Mangrove extent, blue carbon potential and CO_2 emissions in 1996–2020. *Science of The Total Environment, 915,* 170052. https://doi.org/10.1016/j.scitotenv.2024.170052

Rahman, M. A., Islam, K. R., & Rahman, M. M. (2016). Effects of species composition on soil carbon storage and nutrient dynamics in mangrove ecosystems of the Sundarbans, Bangladesh. *Forest Ecology and Management, 368,* 1–10. https://doi.org/10.1016/j.foreco.2016.03.005

Rahman, M. M., Asaduzzaman, M., & Islam, M. S. (2010). Ecosystem-based adaptation to climate change: A case study of the Sundarbans mangrove forest, Bangladesh. *Environment and Natural Resources Research, 1*(1), 1–10. https://doi.org/10.5539/enrr.v1n1p1

Sarker, S. K., Reeve, R., Thompson, J., Paul, N. K., & Matthiopoulos, J. (2019). Are we failing to protect threatened mangroves in the Sundarbans world heritage ecosystem? *Scientific Reports, 9*(1), 1–10. https://doi.org/10.1038/s41598-019-44930-2

Sim, W. D., Lee, J. S., & Park, J. H. (2024). Assessing land cover classification accuracy: Variations in the deep learning context. *Remote Sensing, 16*(5), 842. https://doi.org/10.3390/rs16050842

Tucker, C. J. (1979). Red and photographic infrared linear combinations for monitoring vegetation. *Remote Sensing of Environment, 8*(2), 127–150. https://doi.org/10.1016/0034-4257(79)90013-0

U.S. Geological Survey. (2019). *Using the USGS Landsat surface reflectance data products.* U.S. Department of the Interior. https://www.usgs.gov/